

Irradiation effects of swift heavy ions on palladium films deposited on 6H-SiC substrate

T.T. Thabethe^{a*}, T. Nstoane^{a b}, S. Biira^{a c}, E. G. Njoroge^a, T. T. Hlatshwayo^a, V. A. Skuratov^{d,e,f} and J. B. Malherbe^a

^a *Department of Physics, University of Pretoria, Pretoria, South Africa*

^b *South African Nuclear Energy Corporation SOC Limited.*

^c *Department of Physics, Busitema University, Tororo, Uganda*

^d *1 FLNR, Joint Institute for Nuclear Research, Dubna, Russia*

^e *National Research Nuclear University MEPhI, Moscow, Russia*

^f *Dubna State University, Dubna, Russia*

Abstract

The irradiation effect of swift heavy ions on palladium (Pd) films deposited on 6H-SiC was investigated. The samples were irradiated by Xe²⁶⁺ ions with the energy of 167 MeV at fluences of $1 \times 10^{13} \text{ cm}^{-2}$ and $3 \times 10^{14} \text{ cm}^{-2}$ at room temperature. Phase identification, residual stress and surface morphology were investigated with X-ray diffraction (XRD) and scanning electron microscopy (SEM). The XRD results showed that the as-deposited sample was composed of Pd and SiC with no evidence of a reaction between Pd and SiC. No reaction was observed for the lower irradiation fluence, only an increase in the Pd peak intensities was observed indicating improvement in the crystallinity of the material. A reaction between Pd and SiC forming PdSi and Pd₂Si was observed after irradiation at a fluence of $3 \times 10^{14} \text{ cm}^{-2}$. The stress measurements indicated that the films were having tensile and biaxial stress not exceeding 200 MPa. A decrease in stress values was observed with an increase in irradiation fluence. The surface morphology of the as-deposited was flat and composed of small granules. There was an increase in granule sizes due to irradiation at $1 \times 10^{13} \text{ cm}^{-2}$. Irradiating at $3 \times 10^{14} \text{ cm}^{-2}$ caused grain agglomeration and clustering.

Keywords: Palladium, SiC, Swift heavy ions, Irradiation, Stress

Corresponding author: Thabsile Thabethe, email: Thabsile.Thabethe@up.ac.za, thabby.theo@gmail.com.

1. Introduction

Silicon carbide (SiC) material is used in a number of applications in different fields because of its good chemical, mechanical and electrical properties [1]. The four properties of SiC which set it aside from other materials are: relatively high melting temperature, low neutron capture, high thermal conductivity and the size of its electronic band gap [2]. These properties enables SiC to be used as a structural material in nuclear reactors and in high power electronics [2–5].

SiC Schottky diodes are used in different device fabrication, but cannot be used solely as high temperature hydrogen sensors because they result in high power consumption and potential safety hazard [6]. Thus, the use of semiconductors (SiC) with metals such as palladium is employed. Palladium (Pd) combined with SiC (Pd-SiC diodes) provides promising results for use in high temperature gas sensors [7]. The variation in the Schottky barrier upon hydrogen absorption makes the Pd-SiC contact an effective hydrogen sensor [8,9]. Hydrogen absorption in silicide is low, thus the Pd must remain intact during the operational time to ensure device reliability [2].

In nuclear reactors, such as the high temperature gas cooled reactor (pebble bed modular reactor), specifically in fuel kernel, SiC is the main layer that prevents the release of fission products. There have been some reports on the attack of SiC by Pd leading to the formation of nodules of palladium silicides between the SiC and Pd interface [10,11]. Some papers have even related the attack of SiC by palladium to be the reason why SiC is not able to

retain silver fission product [10,11]. Reports on the interaction between Pd and SiC due to thermal treatment are available, see ref [12–15]. More recently, the effect of irradiation with swift heavy ions (SHI) and annealing of Pd-SiC contacts have been reported [16]. The irradiation of Pd-SiC composites with swift heavy ions will help to comprehend how effective the composite will be when exposed to severe conditions (e.g. those used as hydrogen sensors). Furthermore, information will be gained on whether the Pd and SiC reaction observed in the fuel kernel are enhanced in the presence of irradiation.

There is limited to no information regarding residual stress variations, crystal structure changes and surface modification induced by SHI irradiation of Pd-SiC composites. Residual stress is one of the major factors which contributes to device reliability [17,18]. Properties such as hardness, adhesion, fracture toughness, etc. for deposited films are affected by residual stress [19]. Thus, residual stress can lead to various film failures, including cracking and delamination [19]. Residual stress is normally introduced by thermally induced stress, stress resulting from film growth, externally applied and environmental stresses. Therefore, the focus of this study is on the effect of SHI irradiation on residual stress, structural changes and surface modifications.

2. Experimental Procedure

A semi-insulating 6H-SiC single-crystal wafer was used in this experiment. The wafer was cut into $5 \times 5 \text{ mm}^2$ pieces using a diamond scribe. The $5 \times 5 \text{ mm}^2$ SiC pieces were then chemically cleaned (methanol, HF, deionised water) to remove any contamination and the native oxide layer. Pd films of more than 300 nm were deposited on the 6H-SiC wafers by resistive evaporation at a base pressure of 3.8×10^{-6} mbar, and 9.0×10^{-6} mbar during evaporation at University of Pretoria. The Inficon deposition rate monitor was used to monitor the Pd thickness during the deposition process. The rate of deposition was between

0.1 and 0.4 Å/s until the required thickness of about 385 nm was obtained.

The Pd-SiC samples were then irradiated with swift heavy ions Xe²⁶⁺ at room temperature with an energy of 167 MeV at the Joint Institute for Nuclear Research (JINR), Dubna. The ion fluences were set at 1×10^{13} and 3×10^{14} ions/cm². The Pd-SiC as-deposited and samples irradiated with SHIs were analysed using X-ray diffraction (XRD) for phase identification and stress measurements, as well as scanning electron microscopy (SEM) for morphology examination. A Bruker-AXS D8 Advance diffractometer, equipped with theta-theta goniometer was used for phase identification. X-ray diffraction (XRD) wide angle X-ray Scattering WAXS using a Cu K α radiation source was used for analysis. For stress-strain, the investigations were performed using a Bruker D8 Discover diffractometer equipped with a theta-2theta goniometer. The instrument was operated in a side-inclination mode. A copper tube (energy = 8 keV) operated in point focus mode was used for the analysis. The primary optics included a 0.8 mm collimator mounted to a graphite monochromator, with no optics on the secondary side. To access the full stress tensor, measurements were carried out at three azimuth angles ϕ , i.e. 0, 45 and 90° with a set of 8 tilt angles in steps of 10° measured for each azimuth angle. To access negative tilt angles, each ϕ was rotated by 180°. To ensure high sensitivity, the Pd (222) reflections at 86.62° (2 θ) were selected for the investigations. Measurements were done on two lateral points across the sample surface and the diffracted beam was collected using an area detector, Vantec500. Stress-strain determination was carried out using the manufacturer's proprietary Leptos v6.02 software.

The average crystallite sizes from the XRD pattern were calculated using the Scherrer Equation (1)[20]:

$$B = \frac{\lambda k}{L \cos \theta} \quad (1)$$

where B is the FWHM, λ is the wavelength (1.540 Å), L is the crystal size, θ is the diffraction 2θ angle and k is the peak sharp factor which is about 0.94 for the cubic structure [20].

The surface morphology of the Pd-SiC samples before and after SHI irradiation were analysed using the Zeiss Ultra 55 field emission scanning electron microscope (SEM). The beam used was set at 0.5 kV so as to disclose surface features before and after irradiation.

3. Results and Discussion

3.1 X-ray diffraction (XRD)

Figure 1 shows the XRD pattern of the Pd-SiC samples before and after irradiation. The XRD results showed that the as-deposited sample was composed of Pd and SiC. The observed SiC peaks suggest that the X-rays penetrated through the Pd layer. About eight palladium peaks were present at the 2θ angles of 40.42° , 47.05° , 68.50° , 82.71° , 86.96° , 105.24° , 120.14° and 125.34° and were attributed to (111), (200), (220), (311), (222), (400), (313) and (402) reflections respectively. The Pd peaks were broad due to the nano-particle size effect. SiC peaks were positioned at the 2θ angle at around 35.80° , 36.27° , 75.40° , 75.49° and 109.9° having (105), (101), (201), (003) and (1015) reflections respectively. This shows that the SiC on the as-deposition sample had more than one phase of SiC with different orientation.

After irradiating the sample with Xe^{26+} SHI to a fluence of $1 \times 10^{13} \text{ cm}^{-2}$, the patterns showed a slight change in the intensity of Pd peaks but no new phases formed. The peak area (area under the curve) of the Pd peaks increased after the initial irradiation. The increase in the peak area can be attributed to improvement in the crystallinity of the polycrystalline Pd film when compared to the as-deposited. An increase in crystallinity is associated with increased temperature. To see whether this is feasible, the ion ranges and energy loss for Pd and SiC were calculated using the Monte Carlo computer programme SRIM-2013 [21]. The electronic energy losses for a 167 MeV xenon ion in Pd and SiC are 40.11 keV/nm and 20.40 keV/nm

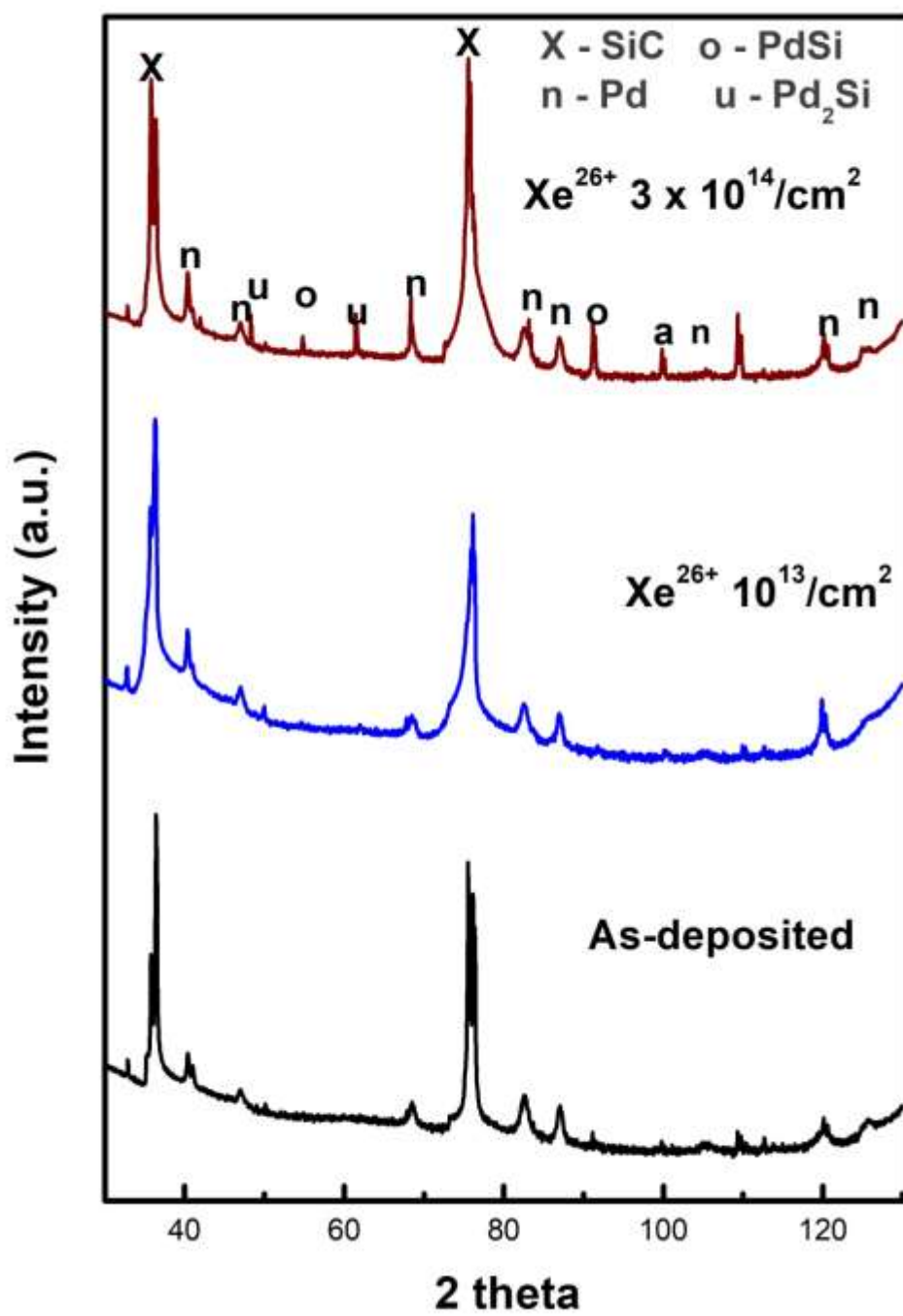


Figure 1: XRD patterns for the Pd-SiC samples before and after irradiation with Xe²⁶⁺ swift heavy ions at room temperature.

respectively, while the nuclear energy losses are 0.210 keV/nm and 0.081 keV/nm respectively. Thus the dominant energy loss mechanism for the incident xenon ions was electronic stopping not nuclear stopping. Based on this energy loss factor, it is evident that the large amount of energy deposited in the Pd film which increased its temperature. It is well-known [22] that the average grain size of a film increases with increasing temperature. This grain growth in the Pd film led to the increase in the XRD Pd peak intensities and corresponding areas.

The SiC double peaks at high scattering angles combined to form one peak at position 76.10° . The broadening on the SiC after irradiated is because of the defects introduced by the irradiation [23]. That is, irradiation causes structural (crystal) rearrangement during the irradiation process thereby introducing defects in the material.

The SiC peak at 109.9° was observed to increase after irradiation at $3 \times 10^{14} \text{ cm}^{-2}$. The increase in the SiC peak at 109.9° after irradiation was probably due to the increase in the sample temperature (large amount of energy deposited during irradiation). That is, irradiation introduces defects in the sample and simultaneously causes defect annealing (due to the change in temperature).

Irradiating the samples to a fluence of $3 \times 10^{14} \text{ cm}^{-2}$ resulted in the appearance of four new peaks. These peaks were identified as PdSi and Pd₂Si. The PdSi peaks were at 2-theta position of 54.18° and 91.15° with (002) and (042) orientations respectively. The Pd₂Si peaks were observed at the 2theta positions of 48.72° and 61.45° with the orientation of (300) and (112) respectively (see Figure 1). This was an indication that a reaction between Pd and SiC had occurred due to SHI irradiation. The formation of Pd₂Si was also observed by Njoroge et al. [16] after irradiating Pd-SiC sample with Xe²⁶⁺ SHI at room temperature to a fluence of $4 \times 10^{14} \text{ cm}^{-2}$. This shows that in the Pd and SiC reaction, Pd₂Si is the favoured product after

irradiating at a fluence of 10^{14} cm^{-2} . In all the cases, the Pd peaks were observed, which suggested that Pd had not fully reacted. Narrowing of and an increase in intensities of the Pd peaks were observed. This was due to further increases in the sizes of the Pd crystallites due to energy deposition of the penetrating xenon ions.

The change in the Pd average crystallite size (grain size) was calculated using the Scherrer equation and the results are tabulated in Table 1. The Pd average crystallite size in the as-deposited was calculated to be 207.5 nm, which increased to 272.2 nm after irradiating at the fluence of $1 \times 10^{13} \text{ cm}^{-2}$. Irradiating the sample at $3 \times 10^{14} \text{ cm}^{-2}$ led to a further increase in the average crystallite size to 316.1 nm. The change in the Pd average crystallite size was due to the irradiation of the sample and the corresponding increase of temperature in the Pd layer as discussed above. This indicates that increasing irradiation fluence enhances crystallite growth.

Table 1: The grain sizes (crystallite sizes) calculated for the phases in the Pd-SiC sample before and after irradiation at different fluences.

Irradiation fluence	Crystallite size (nm)		
	Pd	PdSi	Pd ₂ Si
As-deposited	208		
$1 \times 10^{13} / \text{cm}^2$	272		
$3 \times 10^{14} / \text{cm}^2$	316	119	117

3.2 Residual stress

Stress measurements were performed in order to investigate the effect of irradiation with SHIs on the samples. Tables 2 and 3 depict the stress measurement results obtained from XRD. The results illustrate that the measured stress was tensile and equibiaxial for all the

samples and did not exceed 200 MPa. Overall, the stress measurements tabulated in Table 2, agreed within error bars, suggesting the stress state in the coating was spatially homogenous. Table 3 shows the average stress measured and the change in stress introduced by irradiation (irradiation induced stress) with the as-deposited used as a frame of reference. It is evident from Table 3 that upon initial irradiation, the stress relaxed by ~5% (compared to the as-deposited layer) to 183 MPa. With further irradiation ($3 \times 10^{14} \text{ cm}^{-2}$) it relaxed further to ~174 MPa. This stress reduction is due to the increase in temperature in the Pd film following the swift heavy ion bombardment. This suggests that the radiation-induced stress is compressive (showed by the negative sign on Table 3). The reduction in tensile stress is caused by compressive stress introduced by the irradiation.

Table 2: Residual stress values for the Pd before and after irradiating with swift heavy ions.

Irradiation fluence	Measurement	Stress components (MPa)	
		σ_{11}	σ_{22}
as-deposited	1	192 ± 6	195 ± 6
	2	191 ± 5	193 ± 5
$1 \times 10^{13} / \text{cm}^2$	1	185 ± 6	186 ± 6
	2	182 ± 5	181 ± 5
$1 \times 10^{14} / \text{cm}^2$	1	171 ± 6	175 ± 6
	2	172 ± 5	177 ± 5

Table 3: The average residual stress and actual stress caused by irradiation on Pd compared to the as-deposited.

Irradiation Fluence	σ_{11} (MPa) (Average)	Radiation- Induced σ_{11} (MPa)	σ_{22} (MPa) (Average)	Radiation- Induced σ_{22} (MPa)
As deposited	192 ± 6	0	194 ± 7	0
$1 \times 10^{13} / \text{cm}^2$	183 ± 7	-9	183 ± 8	-11
$3 \times 10^{14} / \text{cm}^2$	172 ± 6	-11	176 ± 7	-7

Stress in thin films usually decreases with increasing temperature for a few reasons. One of these is temperature related grain growth. Grain growth in thin films is governed by minimization of the Gibbs free energy in the film. This is manifested by minimization of the surface, interface and strain energies between the different grains [22]. Thus, the preferential growth of grains is also affected by strain. Grains with different orientations have different strain energy densities. The strain energies contribute to grain growth by increasing the surface energies of the atoms leading to enhanced surface diffusion of the atoms on a particular crystal plane. This favours the growth of grains with minimum strain energy, thereby reducing the stress in the film. Another source of stress in thin films is the stress in grain boundaries. According the Hoffman model [24–26] the grain boundary stress is inversely proportional to the diameter of the grain. Thus, the films with larger grains (i.e. the irradiated films) will have less stress than the as-deposited layer. Furthermore, this temperature increase due to irradiation also annealed some of the defects such as dislocations, interstitials, etc. in the crystallites, thereby, relieving some of the stress in the film.

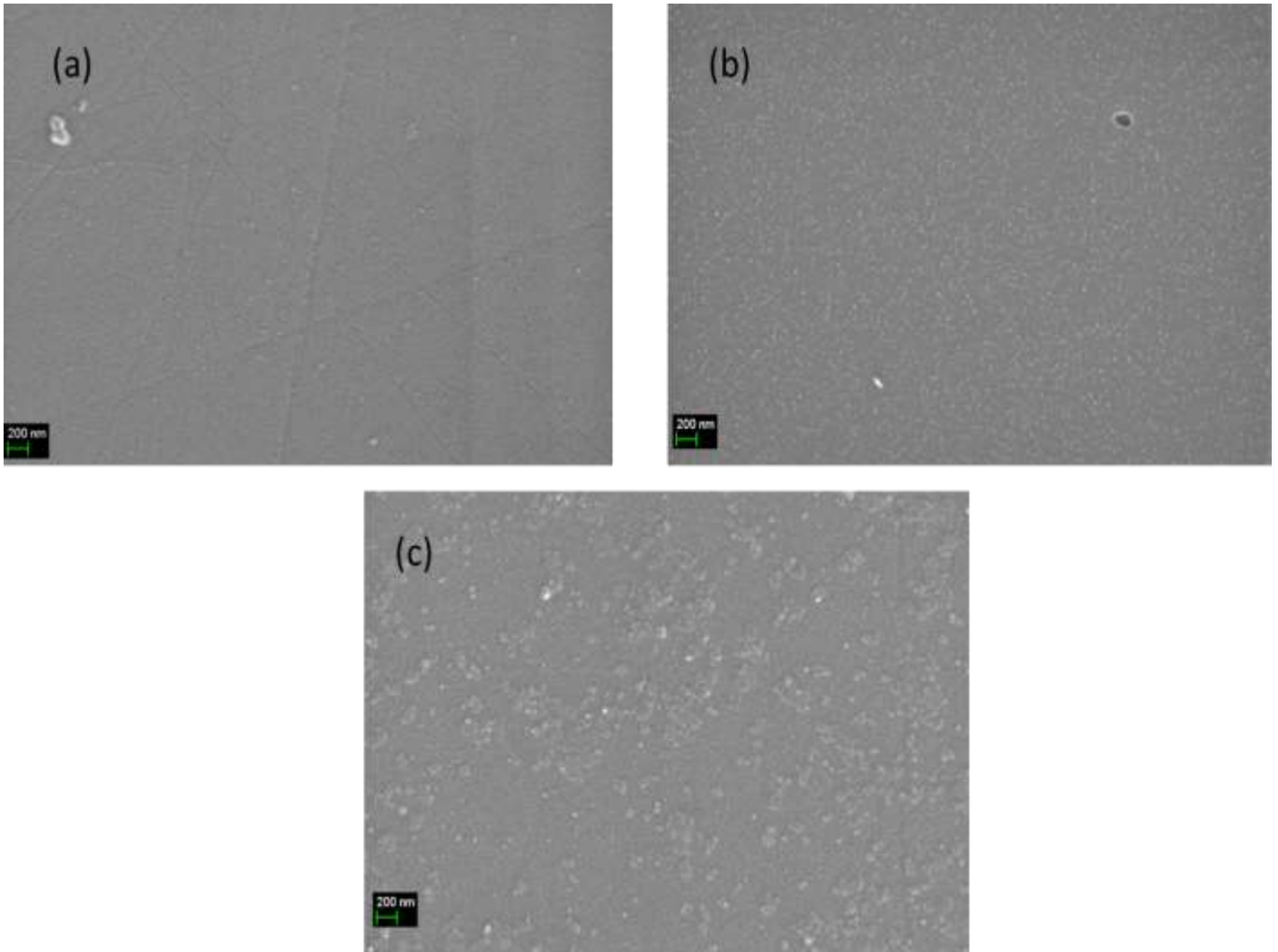


Figure 2: SEM images of the Pd-SiC (a) before and after irradiating them with SHI at fluences of (b) 1×10^{13} ions/cm² and (c) 3×10^{14} ions/cm² at room temperature.

3.3 Scanning electron microscopy (SEM)

To study the near surface morphology, SEM was conducted and the images before and after irradiation are depicted in Figure 2. The as-deposited sample was composed of relatively small Pd crystals (granules) distributed on the SiC surface. The Pd film was uniformly deposited on the SiC substrate. The samples irradiated with SHI to a fluence of 1×10^{13} cm⁻² indicated an increase in the Pd granule sizes after the initial irradiation. The Pd granules were also homogeneously distributed. The sample irradiated with a fluence of 3×10^{14} cm⁻² led to further increase in the granule sizes and grain coarsening. The surface structure exhibited

clustering and agglomeration of the granules. An uneven grain growth throughout the surface was observed to occur with some parts of the surface having a hill-like growth due to the agglomeration and the preferential growth of certain crystal planes in accordance with Wulff's law [27], that is, a crystal surface with a higher surface energy will grow proportionally faster than another surface with a lower surface energy. This increases the surface area with a lower surface energy, consequently the minimizing the total energy of the crystal. This uneven growth mode produces topography on the film surface.

The SEM results are in partial agreement with the XRD results as shown by the increase in Pd intensity peak and increase in the average crystal size due to the irradiation. However, there is a striking difference between the XRD measured grain sizes and the crystal sizes seen in the SEM images. This is due to the grain growth mode in deposited layers on a substrate. It is well-known that the grains in deposited films usually grow in a columnar structure [22]. This is due to the fact that growth of the crystallite can only occur at the top crystal surfaces exposed to the depositing atoms. CVD grown SiC also has a columnar structure [28,29]. Since XRD measures the average crystal sizes, the major contribution to those measurements came from the elongated parts of the grains perpendicular to the film surface. Consequently, grains seen by SEM will be significantly smaller than the values given in Table 1.

4. Conclusions

The effect of swift heavy ions irradiation on thin Pd films deposited on 6H-SiC was studied. The Pd-SiC couple were irradiated at room temperature with 167 MeV Xe²⁶⁺ ions. X-ray diffraction analyses were used for phase identification and residual stress measurements. SEM was conducted to study the surface morphology of the samples. The XRD phase identification results showed that the as-deposited Pd film did not react with the SiC substrate to form any new phases. The SEM indicated that the surface was composed of small Pd

granules and it was fairly flat. The sample irradiated to a fluence of $1 \times 10^{13} \text{ cm}^{-2}$ showed that no reaction between Pd and SiC had occurred but the sample surface showed an increase in granule size and the development of surface topography. The sample irradiated at $3 \times 10^{14} \text{ cm}^{-2}$ indicated that a reaction took place between Pd and SiC forming PdSi and Pd₂Si. The surface topography increased more with clustering and agglomeration of the granules on the sample surface.

The increase in average Pd grain size and increase in surface topography with increasing swift heavy ion bombardment were due to an increase in the temperature in the films. A SRIM simulation showed that the electronic loss by the 167 MeV Xe²⁶⁺ ions in the Pd film was about 40 keV/nm. This large amount deposited energy led to a local increase in temperature in a very short time resulting in solid phase epitaxy to occur on the grain level.

The Pd films before and after irradiation had equibiaxial tensile stress. The average stress for both the σ_{11} and σ_{22} components in the as-deposited Pd films was $193 \pm 6.2 \text{ MPa}$. After 167 MeV Xe²⁶⁺ ion irradiation to a fluence of $1 \times 10^{13} \text{ cm}^{-2}$, the stress relaxed by ~5 % and by ~10% for the higher fluence. The actual stress induced by irradiation was compressive stress, thus a decrease in the tensile stress after irradiation was observed.

5. Acknowledgement

This work is based upon research supported by the National Research Foundation (NRF) (Grant number: 111994 and 110475), South Africa. Any opinion, findings and conclusions or recommendations expressed in this work are those of the authors and the NRF do not accept any liability with regard thereto. T. T. Thabethe acknowledges the financial support from the NRF.

References

- [1] C. Guo, C. Zhang, L. He, B. Jin, N. Shi, Microstructure Characterization of Long W Core SiC Fiber, *J. Mater. Sci. Technol.* 23 (2007) 677–684.
- [2] G. Roma, Palladium in cubic silicon carbide : Stability and kinetics, *J. Appl. Phys.* 106 (2009) 123504.
- [3] E.G. Njoroge, C.C. Theron, J.B. Malherbe, N.G. Van Der Berg, T.T. Hlatshwayo, V.A. Skuratov, Nuclear Instruments and Methods in Physics Research B Surface and interface modification of Zr / SiC interface by swift heavy ion irradiation, *Nucl. Inst. Methods Phys. Res. B.* 354 (2015) 249–254.
- [4] V.B. Shields, application of SiC in high temperature electronics and sensors, NASA Jet Propulsion Laboratory, Tech Briefs 0145-319X, 2015. doi:hdl:2014/31708.
- [5] E. Kalinina, G. Onushkin, D. Davidov, A. Hallin, A. Konstantinog, V.A. Skuratov, Electrical Study of 4H-SiC Irradiated with Swift Heavy Ions, 12th International Conference on Semiconductor and insulating Materials, (2002) 106–109. doi: 10.1109/SIM.2002.1242735
- [6] H. Gu, Z. Wang, Y. Hu, Hydrogen Gas Sensors Based on Semiconductor Oxide Nanostructures, *Sensors*, 12 (2012) 5517-5550 doi:10.3390/s120505517.
- [7] K. Kim, G. Chung, Sensors and Actuators B : Chemical Fast response hydrogen sensors based on palladium and platinum / porous 3C-SiC Schottky diodes, *Sensors Actuators B. Chem.* 160 (2011) 1232–1236.
- [8] C.K. Kim, J.H. Lee, Y.H. Lee, N.I. Cho, D.J. Kim, W.P. Kang, Hydrogen Sensing Characteristics of Pd-SiC Schottky Diode Operating at High Temperature, 28 (1999)

- 202–205.
- [9] Z. Yan, G. He, M. Cai, H. Meng, P.K. Shen, Formation of tungsten carbide nanoparticles on graphitized carbon to facilitate the oxygen reduction reaction, *J. Power Sources*. 242 (2013) 817–823.
- [10] J.H. Neethling, J.H. O’Connell, E.J. Olivier, Palladium assisted silver transport in polycrystalline SiC, *Nucl. Eng. Des.* 251 (2012) 230–234.
- [11] J.H. O’Connell, J.H. Neethling, Palladium and ruthenium supported silver migration in 3C–silicon carbide, *J. Nucl. Mater.* 456 (2015) 436–441.
- [12] J.Y. Veuillen, T.A. Nguyen Tan, I. Tsiaoussis, N. Frangis, M. Brunel, R. Gunnella, Reaction of palladium thin films with an Si-rich 6H-SiC(0001)(3×3) surface, *Diam. Relat. Mater.* 8 (1999) 352–356.
- [13] K. Fu, P.J. Meadows, J. Tan, P. Xiao, Palladium Attack, 4141 (2010) 4135–4141.
- [14] R.L. Pearson, R.J. Lauf, T.B. Lindemer, The interaction of Palladium, the Rare Earths, and Silver with Silicon Carbide in HTGR Fuel Particles, (1982) 1–41.
papers2://publication/uuid/82A41DF5-F86E-4A00-8D9A-EBF703EC69D6.
- [15] G. Roma, Palladium in silicon carbide : indirect diffusion mechanisms from first principles, 123504 (2009) 123504.
- [16] E.G. Njoroge, C.C. Theron, V.A. Skuratov, D. Wamwangi, T.T. Hlatshwayo, C.M. Comrie, et al., Interface reactions between Pd thin films and SiC by thermal annealing and SHI irradiation, *Nucl. Instruments Methods Phys. Res. Sect. B Beam Interact. with Mater. Atoms.* 371 (2016) 263–267.
- [17] A.M. Engwall, Z. Rao, E. Chason, Origins of residual stress in thin films : Interaction

- between microstructure and growth kinetics, *JMADE*. 110 (2016) 616–623.
- [18] Y. Xi, K. Gao, X. Pang, H. Yang, X. Xiong, Film thickness effect on texture and residual stress sign transition in sputtered TiN thin films, *Ceram. Int.* 43 (2017) 11992–11997.
- [19] D. Escobar, R. Ospina, A.G. Gómez, E. Restrepo-parra, Microstructure, residual stress and hardness study of nanocrystalline titanium – zirconium nitride thin films, *Ceram. Int.* 41 (2015) 947–952.
- [20] S. Biira, B.A.B. Alawad, H. Bissett, J.T. Nel, T.P. Ntsoane, T.T. Hlatshwayo, et al., Influence of the substrate gas-inlet gap on the growth rate, morphology and microstructure of zirconium carbide films grown by chemical vapour deposition, *Ceram. Int.* 43 (2017) 1354–1361.
- [21] J.F. Ziegler, Interactions of ions with matter, *Free Softw.* (2015). doi:10.1007/3-540-29471-6_5.
- [22] C.V. Thompson, Structure evolution during processing of polycrystalline films, *Annu. Rev. Mater. Sci.* 3 (2000) 159–190.
- [23] F.D.A. S.M. Tunhuma, M. Diale, J.M. Nel, J. Madito, T.T. Hlatshwayo, Defects in swift heavy ions irradiated n-4H SiC, *Nucl. Instruments Methods Phys. Res. Sect. B-Beam Interact. with Mater. Atoms.* Submitted (2018).
- [24] R.W. Hoffman, Micromechanics of films, fibrils and interfaces-an overview, *Thin Solid Films.* 89 (1982) 155–164.
- [25] F.A. Doljack, R.W. Hoffman, The origins of stress in thin nickel films, *Thin Solid Films.* 12 (1972) 71–74.

- [26] R. W. Hoofman, Stresses in thin films: the relevance of grain boundaries and impurities, *Thin Solid Films*. 34 (1976) 185–190.
- [27] G. Z. Wulf, Zur Frage der Geschwindigkeit des Wachstums und der Auflösung der Krystallflagen, *Krist. Mater.* 34 (1901) 449.
- [28] J.B. Malherbe, N.G. van der Berg, A.J. Botha, E. Friedland, T.T. Hlatshwayo, R.J. Kuhudzai, et al., SEM analysis of ion implanted SiC, *Nucl. Instruments Methods Phys. Res. Sect. B-Beam Interact. with Mater. Atoms*. 315 (2013) 136–141.
- [29] E. Friedland, N.G. van der Berg, J.B. Malherbe, J.J. Hancke, J. Barry, E. Wendler, et al., Investigation of silver and iodine transport through silicon carbide layers prepared for nuclear fuel element cladding, *J. Nucl. Mater.* 410 (2011) 24–31.